ANL-HEP-CP-99-43
NIKHEF 99-012

Detailed Comparison of Next-to-Leading Order Predictions for Jet Photoproduction at HERA

B.W. Harris[a], M. Klasen[a], and J. Vossebeld[b]

[a] Argonne National Laboratory, Argonne, IL, USA
[b] NIKHEF, Amsterdam, the Netherlands

Abstract: The precision of new HERA data on jet photoproduction opens up the possibility to discriminate between different models of the photon structure. This requires equally precise theoretical predictions from perturbative QCD calculations. In the past years, next-to-leading order calculations for the photoproduction of jets at HERA have become available. Using the kinematic cuts of recent ZEUS analyses, we compare the predictions of three calculations for different dijet and three-jet distributions. We find that in general all three calculations agree within the statistical accuracy of the Monte Carlo integration yielding reliable theoretical predictions. In certain restricted regions of phase space, the calculations differ by up to 5%.

1 Introduction

Our present knowledge of the hadronic structure of the photon rests on rather limited data from inclusive deep-inelastic electron-photon scattering. At leading order (LO) of perturbative QCD, the photon structure function $F_2^\gamma(x,Q^2)$ is related to the singlet quark densities (dominated by the up-quark density) which are the only well constrained parton densities in the photon. In contrast, the gluon density in the photon is only constrained theoretically by a global momentum sum rule. Experimental constraints are weak, since the gluon contributes to $F_2^\gamma(x,Q^2)$ only at next-to-leading order (NLO) of QCD. Therefore, the available parametrizations of the photon structure function rely heavily on assumptions like Vector Meson Dominance. Valuable information on the gluon density in the photon is provided by jet photoproduction, where existing data have already ruled out a very large and hard gluon density.

Jet photoproduction has been measured with increasing precision at HERA since the electron-proton collider became operational in 1992. These data make it now possible to discriminate between different parametrizations of the photon structure if uncertainties from the proton structure and from the partonic scattering process can be minimized. The proton structure is well constrained in the relevant regions of x from deep-inelastic HERA data. Direct and resolved photon-proton scattering processes into one or two jets have been calculated by three groups in NLO QCD [1, 2, 3]. These calculations are also applicable to LO three-jet production. The purpose of this paper is to check the consistency of these three calculations using the kinematic cuts of recent ZEUS dijet [4] and three-jet [5] analyses at a precision that is only limited by

the accuracy of the numerical integration. The organization of the paper is as follows: In Sect. 2 we briefly describe the theoretical methods used in the perturbative calculations. In Sect. 3 we present a detailed comparison of the LO three-jet distributions, and in Sect. 4 we present the comparison of the NLO dijet distributions. In Sect. 5 we discuss remaining theoretical and experimental uncertainties, and we give our conclusions in Sect. 6.

2 Theoretical Methods Used in the NLO Calculations

The basic components in current NLO jet photoproduction calculations are $2 \to 2$ body squared matrix elements through one-loop order and tree-level $2 \to 3$ body squared matrix elements, for both photon-parton and parton-parton initiated subprocesses. It is therefore possible to study single- and dijet production at NLO and three-jet production at LO. The goal of the next-to-leading order calculations is to organize the soft and collinear singularity cancellations without loss of information in terms of observable quantities. The methods to accomplish this cancellation can be categorized as the phase space slicing and subtraction methods.

The calculation of [1] uses the subtraction method. In the center of mass frame of the incoming parton the final state parton four vectors may be written as $p_i = \frac{\sqrt{S}}{2}\xi_i(1, \sqrt{1-y_i^2}\vec{e}_{iT}, y_i)$ where $\vec{e}_{iT}$ is a transverse unit vector. By construction, the parton i gets soft when $\xi_i \to 0$, and collinear to the incoming partons when $y_i \to \pm 1$. The n-dimensional three-body phase space written in terms of ξ_i and y_i is proportional to $\xi_i^{1-2\epsilon}(1-y_i^2)^{-\epsilon}$, where $\epsilon = 2 - n/2$. The soft singularities in the matrix element squared, which are of $\mathcal{O}(\xi_i^{-2})$, are regulated by multiplying them by ξ_i^2 and at the same time dividing the phase space by ξ_i^2, resulting in a $\xi_i^{-1-2\epsilon}(1-y_i^2)^{-\epsilon}$ structure. The term $\xi_i^{-1-2\epsilon}$ is replaced by plus distributions and soft poles in ϵ. Within these terms $(1-y_i^2)^{-\epsilon}$ is replaced by additional plus distributions and collinear poles in ϵ. The soft and final state collinear singularities cancel upon addition of the interference of the leading order diagrams with the renormalized one-loop virtual diagrams. The initial state collinear singularities are removed through mass factorization. The result is a finite function of various combinations of plus distributions. The main drawback of this method is that in the subtracted integrals, the numerical singularity cancellation takes place between terms of different kinematics which requires special care.

The calculation of [2] uses a phase space slicing method that employs two small cut-offs δ_s and δ_c to delineate soft and collinear regions of phase space. This avoids partial fractioning at the expense of a somewhat more complicated split of phase space. Defining the four vectors of the three-body scattering process as $p_1 + p_2 \to p_3 + p_4 + p_5$ one takes $s_{ij} = (p_i + p_j)^2$. The soft region is then $E_i < \delta_s\sqrt{s_{12}}/2$ where E_i is the energy of the emitted gluon. In this region one puts $p_i = 0$ everywhere except in denominators of matrix elements, and performs the integral over the restricted phase space in n dimensions. The complementary region, $E_i > \delta_s\sqrt{s_{12}}/2$, is called the hard region. That portion of the hard region satisfying s_{ij} or $|t_{ij}| < \delta_c s_{12}$ with $t_{ij} = (p_i - p_j)^2$ is treated with collinear kinematics and is also integrated in n dimensions. The poles in ϵ cancel as described above, and terms of order δ_c and δ_s are neglected compared to double and single logarithms of the cut-offs. The hard and non-collinear phase space region is integrated numerically. The sum is independent of the cut-offs provided they are chosen small enough. This serves as a useful check on results.

The calculation of [3], which is also of the phase space slicing type, uses an invariant mass cut to isolate singular regions of phase space. The $2 \to 3$ body squared matrix elements are

partially fractioned to separate overlapping soft and collinear singularities. As above one defines $s_{ij} = (p_i + p_j)^2$. In the situation when $s_{ij} \leq y s_{12}$ the partons i and j cannot be resolved. In this region the phase space integrals are performed in n dimensions which produces double and single poles in ϵ. They cancel as described above. Terms of order y are neglected in the process, but double and single logarithms in y are retained. The region $s_{ij} > y s_{12}$ is integrated numerically. The sum is independent of y provided it is chosen small enough. As above, this serves as a useful check on results.

The final result of these calculations is an expression that is finite in four-dimensional space-time. One can compute all phase space integrations using standard Monte-Carlo integration techniques. The result is a program which returns parton kinematic configurations and their corresponding weights, accurate to $\mathcal{O}(\alpha\alpha_s^2)$. The user is free to histogram any set of infrared-safe observables and apply parton level cuts, all in a single histogramming subroutine. The calculations have the added benefit that when one considers a manifestly three-body observable the two body contributions don't contribute and a leading order three-jet prediction results.

3 Three-Jet Cross Sections

During 1995 and 1996, positrons of energy $E_e = 27.5$ GeV were collided at HERA with protons of energy $E_p = 820$ GeV. In ZEUS photoproduction events were selected by anti-tagging the positron such that the photon has a virtuality Q^2 smaller than 1 GeV^2 and an energy fraction in the positron $0.2 < y < 0.8$. Three-jet events were analysed with a k_T clustering algorithm using a jet separation parameter of $R = 1$ in a rapidity range of $|\eta| < 2.4$. The jets were required to have transverse energies above 6 GeV (two highest E_T jets) and above 5 GeV (third jet). Additional cuts were placed on the three-jet mass $M_{3-\text{jet}} > 50$ GeV, the leading jet energy fraction $x_3 < 0.95$, and the cosine of the leading jet scattering angle $|\cos\theta_3| < 0.8$ [5]. NLO calculations for three-jet photoproduction are not yet available, so the theoretical predictions for three-jet distributions, which are compared here, are only accurate to LO. Therefore one tests only the $2 \to 3$ phase space generators and the tree-level $2 \to 3$ matrix elements, but no soft or collinear singular regions. All calculations use CTEQ4L [6] and GRV-LO [7] parton distributions in the proton and photon, respectively. The strong coupling constant $\alpha_s(\mu)$ is calculated in leading order with five flavors and $\Lambda^{(5)}_{\text{QCD}} = 181$ MeV, and the renormalization and factorization scale μ is identified with the largest transverse energy of the three jets.

In Fig. 1 we compare the theoretical predictions for the LO three-jet mass distribution by Harris and Owens (HO) and by Frixione and Ridolfi (FR) to those by Klasen and Kramer (KK). In the upper figure we plot the absolute cross section which falls exponentially with $M_{3-\text{jet}}$. This demonstrates that the total cross section is dominated by the region close to $M_{3-\text{jet}} > 50$ GeV. In the lower figure we plot the relative difference between the results by HO and by FR to the results by KK, normalized to the latter. The statistical accuracy of the different calculations is comparable. It has been included in the error bars and decreases simultaneously with the magnitude of the cross section. The calculation of HO presented here differs from the previous results as published in [5], where the E_T cuts were applied to energy, not transverse energy, ordered jets. It now agrees very well (better than 0.5% at low $M_{3-\text{jet}}$) with that by KK. The calculation by FR is systematically 2% lower.

A similar comparison for the distributions in the energy fractions of the leading and next-to-leading jets is shown in Fig. 2. These distributions are dominated by the available phase space,

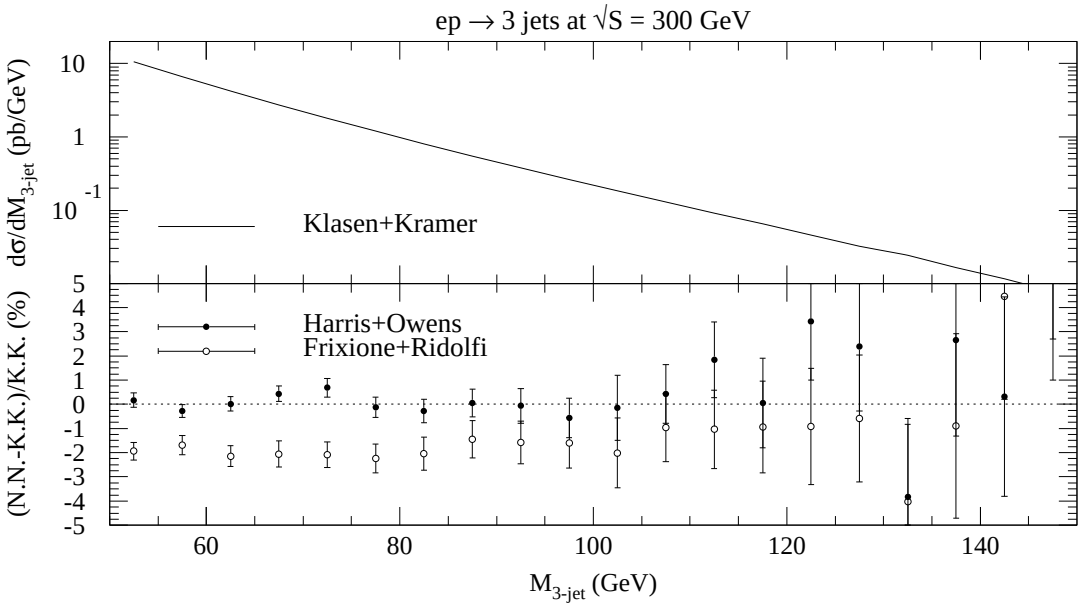

Figure 1: Comparison of three theoretical predictions for the LO three-jet cross section as a function of the three-jet mass $M_{3-\mathrm{jet}}$. The cross section falls exponentially with $M_{3-\mathrm{jet}}$. HO agree very well with KK, whereas FR are systematically 2% lower.

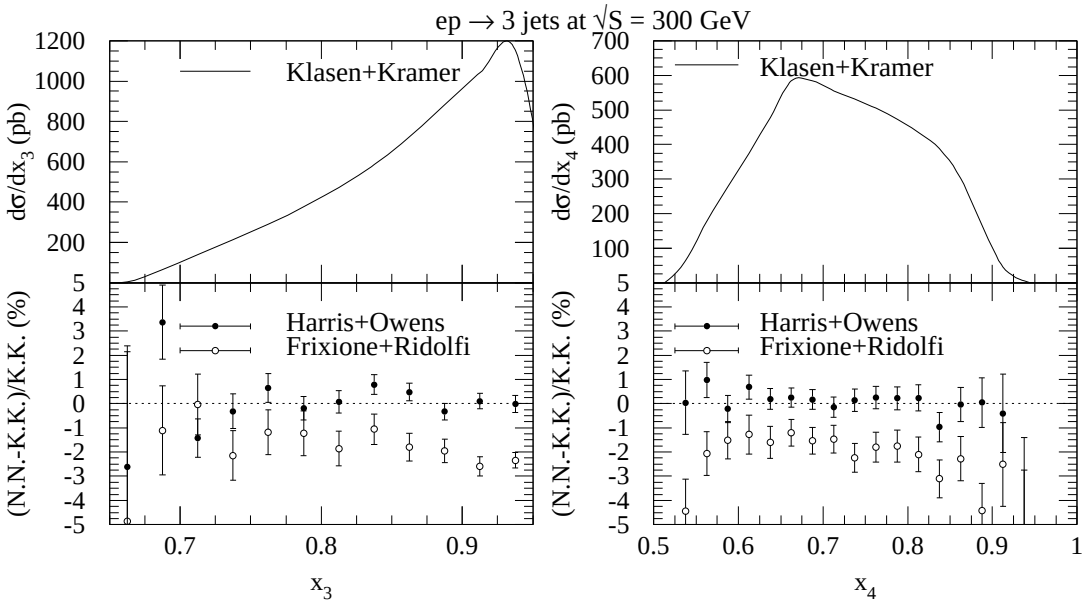

Figure 2: Comparison of three theoretical predictions for the LO three-jet cross section as a function of the energy fractions x_3 (left) and x_4 (right) of the leading and next-to-leading jets. The distributions are dominated by the available phase space. HO agree very well with KK, whereas FR are systematically 2% lower.

not the QCD dynamics, and thus present a test on the two-to-three phase space generators of the numerical programs. The statistical accuracy depends again on the size of the cross section. Where the cross section is large, HO agree with KK to better than 0.5%. FR are

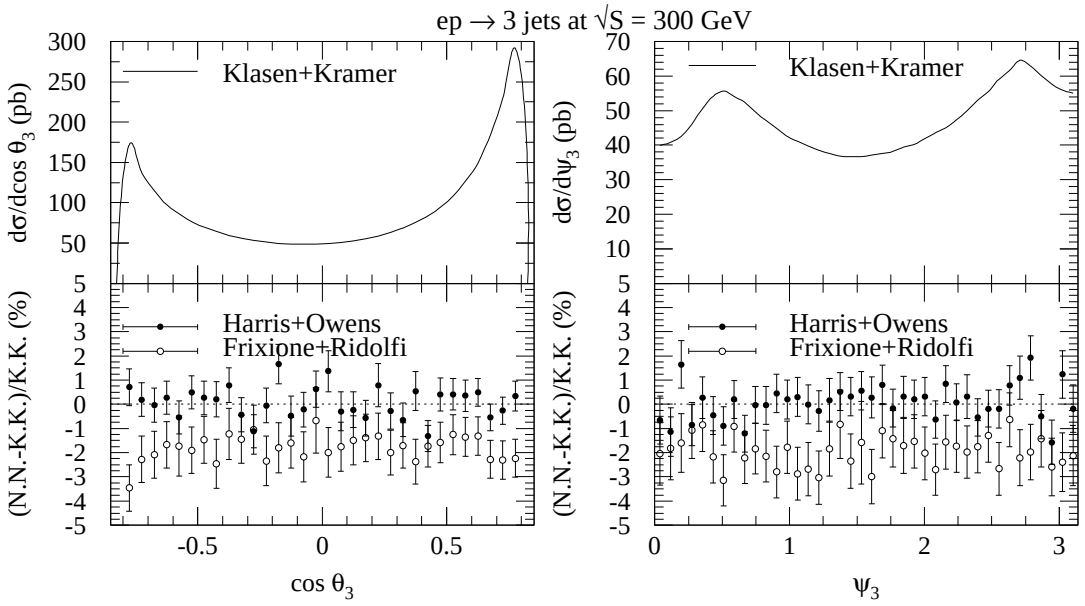

Figure 3: Comparison of three theoretical predictions for the LO three-jet cross section as a function of the cosine of the fastest jet scattering angle $\cos\theta_3$ (left) and the angle ψ_3 between the three jet plane and the plane containing the leading jet and the average beam direction (right). The distributions are sensitive to the pole structure of the QCD matrix elements. HO agree very well with KK, whereas FR are systematically 2% lower.

again 2% lower, which indicates that the difference may come from the phase space generator or kinematic cuts.

The QCD matrix elements are tested in distributions of the cosine of the fastest jet scattering angle $\cos\theta_3$ and the angle ψ_3 between the three-jet plane and the plane containing the leading jet and the average beam direction. The results are presented in Fig. 3. We find again very good agreement between HO and KK and a 2% difference with FR.

4 Dijet Cross Sections

For the dijet photoproduction analysis ZEUS selected again photons with a virtuality below 1 GeV^2. The range of the energy fraction of the photon in the positron $0.2 < y < 0.85$ was slightly larger than in the three-jet analysis, and in addition a narrower band of $0.5 < y < 0.85$ was analyzed which enhances the sensitivity to the parton densities in the photon. The transverse energy of the leading (second) jet was required to be larger than 14 (11) GeV with both jets lying in the rapidity region of $-1 < \eta_{1,2} < 2$ [4]. All NLO calculations use the CTEQ4M and GRV-HO parton densities for the proton and photon and $\Lambda^{(5)}_{\rm QCD} = 202$ MeV corresponding to CTEQ4M in the NLO approximation of $\alpha_s(\mu = \max(E_{T_{1,2}}))$.

In Fig. 4 we compare the theoretical predictions for the NLO dijet cross section as a function of the transverse energy E_T of leading jet with both jets at central pseudorapidities $0 < \eta_{1,2} < 1$. The three calculations agree within the statistical accuracy. The errors are comparable for all three calculations. They are about $\pm 1\%$ ($\pm 2\%$) at low E_T in the full (high) y regime and larger at high E_T due to the steeply falling cross section.

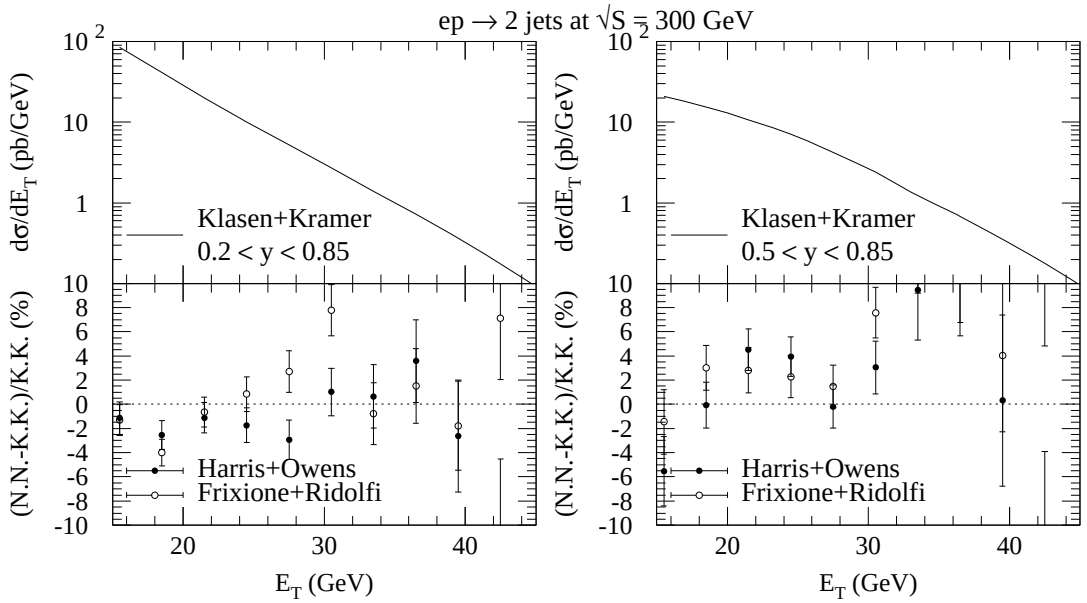

Figure 4: Comparison of three theoretical predictions for the NLO dijet cross section as a function of the transverse energy E_T of the leading jet for the full (left) and high (right) y range. Both jets lie in a central rapidity range $0 < \eta_{1,2} < 1$. The cross sections fall steeply with E_T which leads to increasing statistical errors. All three calculations agree within the statistical accuracy which is about $\pm 1\%$ at low E_T for the full y range and $\pm 2\%$ for the high y range.

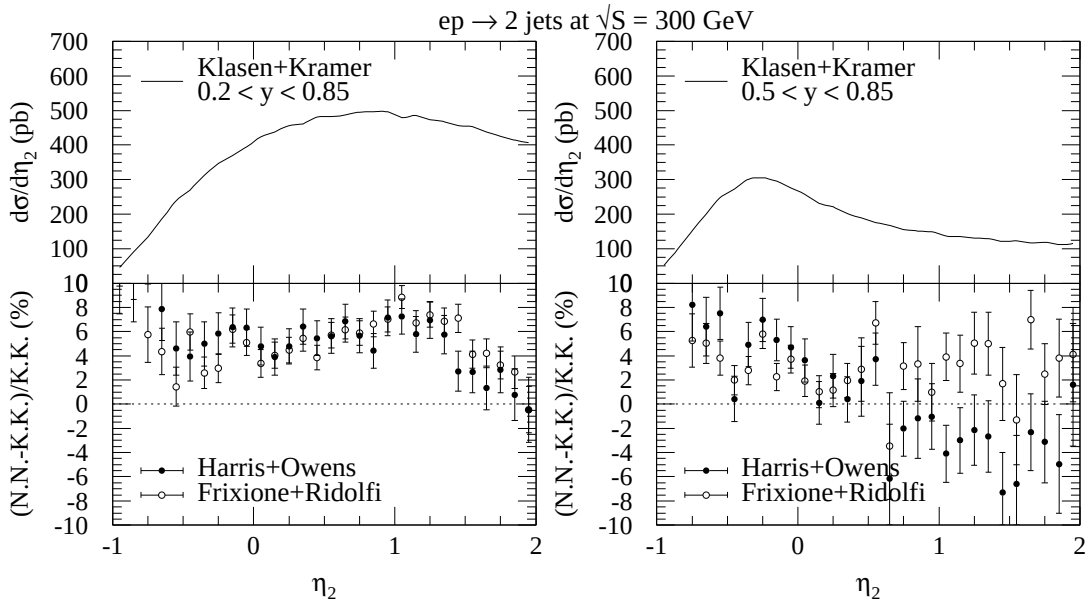

Figure 5: Comparison of three theoretical predictions for the NLO dijet cross section as a function of rapidity η_2 for the full (left) and high (right) y range. The other jet lies in a central rapidity range of $0 < \eta_1 < 1$.

In Fig. 5 we present rapidity distributions for the NLO dijet cross section with a central

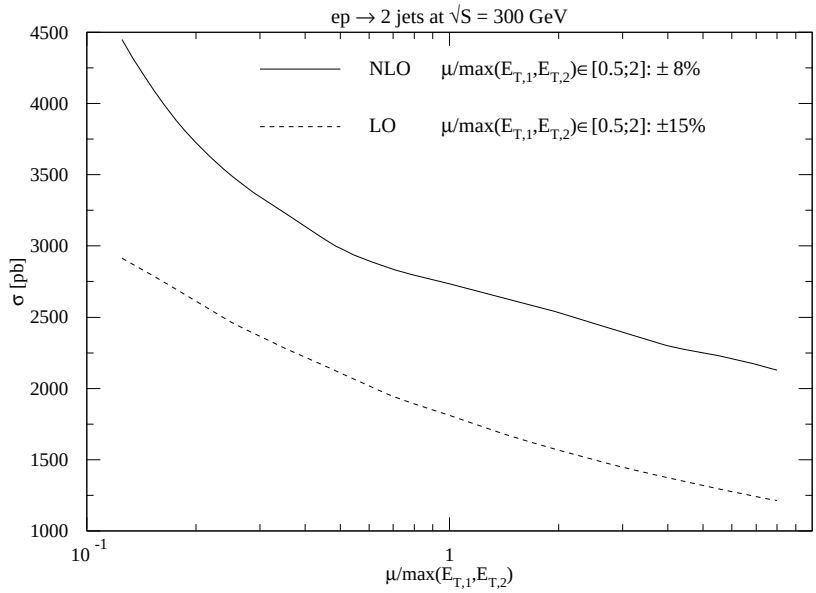

Figure 6: Dependence of the total dijet cross section on the common renormalization and factorization scale μ. The NLO dependence is reduced with respect to the LO dependence, but is still not negligible.

first jet $\eta_1 \in [0;1]$. HO agree with FR for the full y range and are about 5% higher than KK. In the high y range, FR are about 4% higher than KK, whereas HO have a slope from +4% in the backward direction to -4% in the forward direction. Studies have shown that HO agree with KK very well for the resolved processes and for the Born and virtual direct processes. This indicates that the difference, which is still under study, may come from the real direct processes. Within the statistical accuracy of about $\pm 2\%$ the overall agreement is, however, still acceptable.

5 Remaining Uncertainties

The main remaining theoretical uncertainties arise from the dependence of the hadronic cross section on the renormalization and factorization scale μ. This scale dependence is an artifact of the truncation of the perturbative series at next-to-leading order. The scale μ has to be larger than $\mathcal{O}(\Lambda_{\rm QCD})$ to ensure the applicability of perturbation theory. Although the scale μ is in principle arbitrary and the renormalization and factorization scales need not be equal, the logarithmic NLO corrections can be made small by choosing a common scale μ of the order of the hard scattering parameter. In jet photoproduction, the relevant large scales are the transverse energies of the jets E_{T_i} which need not be equal in NLO QCD. This justifies the choice of $\mu = \max(E_{T_i})$ which we have used consistently throughout this paper.

It is customary to estimate the theoretical uncertainty of perturbative calculations by varying μ around the central scale. The dependence of the total dijet cross section with the same kinematic cuts as before on the scale μ is plotted in Fig. 6. We have checked that the calculations by HO and KK agree very well. The LO cross section depends strongly and logarithmically on μ through the strong coupling constant $\alpha_s(\mu)$ and the parton densities in the photon $f^{\gamma}_{q,g}(x_\gamma, \mu^2)$

and proton $f^p_{q,g}(x_p, \mu^2)$. The dependence is reduced in NLO due to explicit logarithms in the virtual and real corrections. However, it still amounts to a considerable uncertainty of about $\pm 8\%$ which can be traced back to the photon factorization scale dependence of the NLO resolved contribution. Whereas the LO photon factorization scale dependence is almost completely cancelled by the NLO direct contribution, the same cancellation for the NLO resolved contribution would require the next-to-next-to-leading order (NNLO) direct contribution which is unknown. The three-jet cross section is only accurate to LO QCD and suffers from even larger scale uncertainties. They have been estimated to be about a factor of two [8].

Further uncertainties arise from the power corrections in the Weizsäcker-Williams approximation [9]. The non-logarithmic terms have been included in all of our numerical results. Although power corrections of $\mathcal{O}(m_e^2/Q^2)$ could be expected to be negligible, an omission of these terms results in an increase in the dijet and three-jet cross section of about 5%. The remaining uncertainty beyond this $\mathcal{O}(m_e^2/Q^2)$ correction is of $\mathcal{O}(\theta_e^2, m_e^2/E_e^2)$ and thus small.

While theoretical calculations are on the parton level, experiments measure hadronic jets. For LO three jet cross sections, every parton corresponds to a jet, making it impossible to implement an experimental jet definition in the theoretical calculation. For NLO dijet cross sections, every jet consists of one or two partons, and a jet definition can be implemented. The cone algorithm suffers from uncertainties with R_{sep}, which are absent in the k_T algorithm used here [10].

Although jet cross sections are mainly sensitive to the dynamics of the hard subprocess, the measured cross sections will at some level be effected by hadronization. These effects are expected to become smaller when the cross section refers to higher transverse energy jets. We have estimated hadronization effects based on the leading order Monte Carlo models HERWIG 5.9 [11] and PYTHIA 5.7 [12]. The jet cross section for hadrons in the final state was compared to the cross section of the partons produced from leading order matrix elements and parton showers (see Fig. 7). In HERWIG the change in the cross section due to fragmentation was found to be less than 10% in most of the kinematic regime. Only for events with one or more very backward jets ($\eta^{jet} < -0.5$) was a more sizeable change observed. For these events the cross section is reduced by up to 40% due to fragmentation. In PYTHIA the reduction of the cross section is much smaller, but shows the same trend. In a related study, presented in [2], HERWIG 5.9 was used to compare the cross section for the final state hadrons to that for the partons of the leading order matrix elements. The relative difference between these cross sections was found to be less than 20%, except again for events with very backward jets ($\eta^{jet} < -0.5$), where the change in the cross section can be as large as 50%. For the three jet measurement, a study of fragmentation effects using PYTHIA 5.7 was presented in [13]. The three jet cross section based on the hadrons in the final state was compared to that of the partons produced in the hard subprocess and the parton showers. The cross section for hadrons was found to be approximately 5% lower than that for partons.

The experimental uncertainty on the dijet cross section is dominated by systematic uncertainties up to transverse jet energies of approximately 25 GeV, depending on the angles of the jets. At higher transverse energies statistical uncertainties dominate. The systematic uncertainties are roughly between 10 and 20% [4]. The experimental uncertainty in the three jet measurement is dominated by systematics up to a three jet mass of approximately 100 GeV and statistics dominated at higher masses. Here, the systematic uncertainties are of the order of 20% [5, 13].

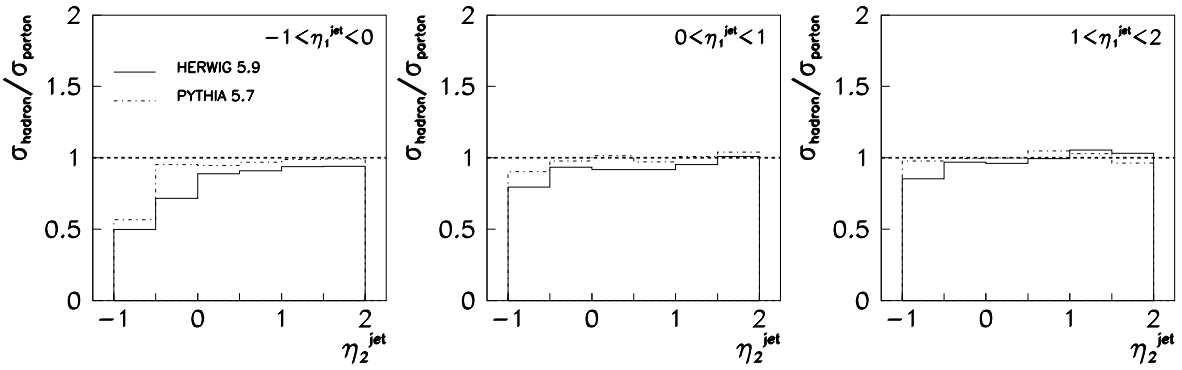

Figure 7: The ratio between the dijet cross section based on hadrons and that based on partons as predicted by HERWIG 5.9 and PYTHIA 5.7. The ratio is given for the cross section as a function of the pseudorapidity of one of the jets while the other jet is restricted to the pseudorapidity range, indicated in the figure.

These measurements correspond to luminosities of 6.3 and 16 pb^{-1}, respectively. Up to the beginning of 1999 the HERA experiments have each collected around 50 pb^{-1}. When these data are used to repeat the discussed measurements, it will be possible to reduce the statistical uncertainties significantly and to extend the measurement to higher transverse energies and masses. Moreover, it is likely that the increase in statistics can be exploited to reduce the systematic uncertainties as well. For the dijet analysis, it was estimated that, when using all available data, statistical uncertainties should dominate the measurement only above transverse energies of approximately 50 GeV, again depending on the angles of the jets. In the long term, after the luminosity upgrade planned in the year 2000, HERA is aiming to deliver about 250 pb^{-1} of luminosity each year. This will allow for the measurement of jet photoproduction cross sections up to still higher transverse energies and masses.

6 Conclusions

We have presented a detailed comparison of three theoretical predictions for LO three-jet and NLO dijet cross sections as measured recently by ZEUS. We found that in general all three calculations agree within the statistical accuracy of the Monte Carlo integration. In certain restricted regions of phase space, the calculations differ by up to 5%. We briefly discussed remaining theoretical and experimental uncertainties and future developments.

Acknowledgments

Work in the High Energy Physics Division at Argonne National Laboratory is supported by the U.S. Department of Energy, Division of High Energy Physics, under Contract W-31-109-ENG-38. Work at NIKHEF is supported by the Dutch Foundation for Research on Matter (FOM). The FR results were produced by us, and we thank Stefano Frixione for assistance with his computer code.

References

[1] S. Frixione, Nucl. Phys. **B507**, 295 (1997) and S. Frixione and G. Ridolfi, Nucl. Phys. **B507**, 315 (1997).

[2] B.W. Harris and J.F. Owens, Phys. Rev. **D56**, 4007 (1997) and Phys. Rev. **D57**, 5555 (1998).

[3] M. Klasen and G. Kramer, Z. Phys. **C76**, 67 (1997) and M. Klasen, T. Kleinwort and G. Kramer, Eur. Phys. J. Direct **C1**, 1 (1998).

[4] J. Breitweg *et al.* [ZEUS Collaboration], DESY 99-057.

[5] J. Breitweg *et al.* [ZEUS Collaboration], Phys. Lett. **B443**, 394 (1998).

[6] H.L. Lai *et al.*, Phys. Rev. **D55**, 1280 (1997).

[7] M. Glück, E. Reya and A. Vogt, Phys. Rev. **D45**, 3986 (1992) and Phys. Rev. **D46**, 1973 (1992).

[8] M. Klasen, Eur. Phys. J. **C7**, 225 (1999).

[9] S. Frixione, M.L. Mangano, P. Nason and G. Ridolfi, Phys. Lett. **B319**, 339 (1993).

[10] J.M. Butterworth, L. Feld, M. Klasen and G. Kramer, Proceedings of the Workshop on "Future Physics at HERA", Hamburg, Germany, May 1996, p. 554, hep-ph/9608481.

[11] G. Marchesini, B.R. Webber, G. Abbiendi, I.G. Knowles, M.H. Seymour and L. Stanco, Comput. Phys. Commun. **67**, 465 (1992) and hep-ph/9607393.

[12] H. Bengtsson and T. Sjöstrand, Comput. Phys. Commun. **46**, 43 (1987) and T. Sjöstrand, Comput. Phys. Commun. **82**, 74 (1994).

[13] E.J. Strickland, Ph.D. Thesis, University of Glasgow (1998).